Long non-coding RNA H19 promotes cell proliferation and invasion by acting as a ceRNA of miR-138 and releasing EZH2 in oral squamous cell carcinoma

YONGLONG HONG[1*], HAITAO HE[2*], WEN SUI[1], JINGGE ZHANG[1], SHENFU ZHANG[2] and DAJIANG YANG[1]

[1]Department of Oral and Maxillofacial Surgery, Shenzhen Hospital of Southern Medical University, Shenzhen, Guangdong 518100; [2]Department of Oral and Maxillofacial Surgery, Daping Hospital, The Third Military Medical University, Chongqing 400042, P.R. China

Received July 28, 2017; Accepted November 29, 2017

DOI: 10.3892/ijo.2018.4247

Abstract. Long non-coding RNAs (lncRNAs) have been shown to play pivotal roles in various types of human cancer, including oral squamous cell carcinoma (OSCC). However, the potential mechanisms of action of lncRNAs in OSCC remain to be fully elucidated. The aim of the present study was to further explore the potential mechanisms of action of lncRNAs in OSCC. We first analyzed Gene Expression Omnibus (GEO) datasets to investigate aberrantly expressed lncRNAs which may be involved in the development of OSCC. Reverse transcription-quantitative PCR (RT-qPCR) was performed to analyze the expression levels of lncRNA H19. In addition, the correlation between H19 expression and the clinical characteristics and prognosis of patients with OSCC was statistically analyzed. The effects of H19 expression on OSCC cells were examined by using overexpression and RNA interference approaches *in vitro* and *in vivo*. To examine the competitive endogenous RNA (ceRNA) mechanisms, bioinformatics analysis and luciferase reporter assay were performed. In addition, the correlation between H19 and microRNA (miR)-138 was detected. H19 was found to be upregulated in OSCC tissues and its high expression level was associated with the TNM stage and nodal invasion, and also correlated with a shorter overall survival of patients with OSCC. The knockdown of H19 significantly inhibited OSCC cell proliferation, migration, invasion and epithelial-mesenchymal transition (EMT), and induced apoptosis *in vitro*; it also suppressed subcutaneous tumor growth *in vivo*. In addition, H19 was found to regulate the expression of oncogene enhancer of zeste homolog 2 (EZH2) by competing with miR-138; the inhibition of miR-138 attenuated the inhibitory effects of H19 knockdown on OSCC cells. On the whole, our findings suggest that H19 functions as an oncogene by inhibiting miR-138 and facilitating EZH2 expression in OSCC. Thus, lncRNA H1 may represent a potential therapeutic target for OSCC.

Correspondence to: Dr Wen Sui, Department of Oral and Maxillofacial Surgery, Shenzhen Hospital of Southern Medical University, 1333 Xinhu Road, Bao'an, Shenzhen, Guangdong 518100, P.R. China
E-mail: wens27@163.com

*Contributed equally

Key words: oral squamous cell carcinoma, long non-coding RNA H19, mircoRNA-138, enhancer of zeste homolog 2

Introduction

Oral squamous cell carcinomas (OSCC) is one of the most common types of cancer, and its incidence is increasing worldwide (1). In spite of considerable advances being made in diagnostics and treatment, the 5-year survival rate for patients with OSCC has not improved during the past few decades and remains <50% (2). Although much scientific research has indicated that local recurrence and nodal metastasis are the major causes of mortality in patients with OSCC, the precise molecular mechanisms remain unclear (3-5). Therefore, in order to improve the diagnosis and management of patients with OSCC, it is important to identify effective diagnostic biomarkers and therapeutic targets.

The mammalian genome encodes large numbers of non-coding transcripts that have structural, regulatory or unknown functions (6,7). Long non-coding RNAs (lncRNAs), a class of transcripts >200 nucleotides in length, have been shown to play significant regulatory roles in epigenetic modulation, as well as transcriptional and post-transcriptional in recent years (8,9). Increasing evidence has indicated that lncRNAs participate in the biological processes of cell proliferation, differentiation, apoptosis and cancer metastasis during cancer development and progression (10-12). However, whether such distinct functions of lncRNAs are involved in the development of OSCC remains unknown. H19 a 2.3 kb of lncRNA molecule which is one of the earliest identified imprinted genes (13). Previous studies have reported that H19 is aberrantly expressed in human cancers, including hepatocellular carcinoma, as well as bladder and breast cancers, and usually correlates with cancer progression, metastasis and a poor prognosis, suggesting that H19 may be used as a biomarker for the diagnosis of these types of cancer (14,15). Moreover, H19 has been found to promote

epithelial-mesenchymal transition (EMT) by antagonizing the activity of microRNAs (miRNAs or miRs) as a competing endogenous RNA (ceRNA), and regulating expression of their downstream genes in several type of cancer, such as pancreatic and colorectal cancer (16,17). Recently, H19 was found to be associated with the risk of OSCC in a Chinese population (18). Zhang *et al* also demonstrated that H19 played a crucial role in the progression of tongue squamous cell carcinoma (TSCC) by regulating the expression of β-catenin and glycogen synthase kinase (GSK)-3β via enhancer of zeste homolog 2 (EZH2), indicating that the inhibition of H19 may be a potential target for the treatment of TSCC (19). However, the roles and mechanism of H19 in the development and progression of OSCC remain to be elucidated.

miRNAs are a class of endogenous small non-coding RNAs, 20-25 nucleotides in length, which can suppress gene expression by directly binding to the 3'-untranslated region (3'-UTR) of target messenger RNAs (mRNAs) to induce mRNA decay or translational repression (20). Several deregulated miRNAs have also been reported in OSCC, and are involved in OSCC cell growth, apoptosis, migration and invasion (21,22). Xu *et al* found that miR-138 was significantly downregulated in OSCC and the overexpression of miR-138 inhibited cell proliferation OSCC *in vitro* and *in vivo* (23). However, to date, at least to the best of our knowledge, there are limited studies available on the association between lncRNAs and miRNAs and their role in the development of OSCC; thus, studies are required to shed further insight into this matter.

In the present study, we first analyzed GEO datasets to investigate aberrantly expressed lncRNAs, and found that H19 was significantly upregulated both in OSCC tissues and cell lines. Moreover, the knockdown of H19 inhibited OSCC proliferation and invasion *in vitro*, and suppressed tumor growth *in vivo*. Finally, H19 was found to play an oncogenic role in OSCC cells by regulating EZH2 and by targeting miR-138. These findings provide a novel mechanism of the H19/miR-138/EZH2 axis in OSCC, and suggest that this axis may be a promising molecular therapeutic target for OSCC.

Materials and methods

Cell lines and tissue samples. Six OSCC cell lines SCC-4 (Cat. no. CRL-1624), SCC-15 (Cat. no. CRL-1623), CAL-27 (Cat. no. CRL-2095) [all from American Type Culture Collection (ATCC), Manassas, VA, USA], HSC-3 (RCB1975), HSC-2 (RCB1945) (both from Riken Cell Bank, Tsukuba, Japan) and Ca9-22 (JCRB0625) [from the Japanese Collection of Research Bioresources (JCRB), Osaka, Japan] were used in this study. All cells were cultured in Dulbecco's modified Eagle's medium (DMEM). The medium was supplemented with 10% fetal bovine serum (FBS; Sigma-Aldrich, St. Louis, MO, USA), 100 U/ml penicillin and 100 μg/ml streptomycin at 37˚C in a 5% CO_2 atmosphere. A non-tumorigenic immortalized oral keratinocyte line (HOK-16B, generous gift from Dr No-Hee Park, University of California, Los Angeles, CA, USA) was maintained in oral keratinocyte medium, supplemented with 1% keratinocyte growth factor plus epithelial growth factor mixture (Invitrogen, Carlsbad, CA, USA). A total of 42 freshly frozen OSCC tissues, as well as 42 matched controls were obtained from the Department of Oral and Maxillofacial Surgery, Shenzhen Hospital of Southern Medical University, Shenzhen, China. None of the patients with OSCC had received radiotherapy or chemotherapy prior to surgery. This study protocol conformed to the Ethics Committee of Shenzhen Hospital of Southern Medical University (Shenzhen, China). All human materials were obtained with informed consent and approved by the Ethics Committee of Shenzhen Hospital of Southern Medical University.

lncRNA expression profile data from GEO. The microarray data was downloaded from the open GEO database (https://www.ncbi.nlm.nih.gov/geo/) and the GEO accession number is GSE3524 (24). These microarray expression data were analyzed by GEO2R bioinformatics software (http://www.ncbi.nlm.nih.gov/geo/geo2r/), which can analyze any GEO series. The adjusted P-values (adj. P-value) using the Benjamini and Hochberg (BH) false discovery rate (FDR) method by default were applied to correct for the occurrence of false-positive results. An adj. $P<0.05$ and a $|logFC|\geq 1$ were set as the cut-off criteria. A heatmap of the 49 lncRNAs which the most significant differences in expression was generated using the online tool Morpheus (https://software.broadinstitute.org/morpheus/).

RNA extraction, reverse transcription and quantitative RT-PCR. For lncRNA analysis, total RNA was isolated from the cells and tissues using TRIzol reagent (Invitrogen) according to the manufacturer's instructions and reverse transcribed using the Superscript III first strand synthesis system (Life Technologies, Carlsbad, CA, USA). For miRNA analysis, RNA was extracted from the liver tissues using the miRNeasy mini kit (Qiagen, West Sussex, UK) according to the manufacturer's instructions. The RNA was then reverse transcribed into cDNA. Amplifications were carried out on an ABI 7500 Real-Time PCR system (Life Technologies) using SYBR-Green according to the manufacturer's instructions. Glyceraldehyde 3-phosphate dehydrogenase (GAPDH) or U6 snRNA were used as endogenous controls. Data were analyzed using 7500 software v.2.0.1 (Applied Biosystems, Foster City, CA, USA), and calculated using the $2^{-\Delta\Delta Cq}$ method (25). All experiments were performed in triplicate.

Cell transfection. The miR-138 mimic, miR-138 inhibitor, mimics negative control (mimics NC) and inhibitor NC were purchased from RiboBio Co., Ltd. (Guangzhou, China). A small interfering RNA against H19 (si-H19) and si-Scramble were purchased from Santa Cruz Biotechnology (Santa Cruz, CA, USA). Plasmid cDNA-H19 was constructed by introducing a *Bam*HI-*Eco*RI fragment containing the H19 cDNA into the same site in the pcDNA3.1 plasmid (Invitrogen). Cell transfections with si-H19, pcDNA-H19 and miR-138 mimic and inhibitor were performed as previously described (26). The HSC-2 and Ca9-22 cells were transfected with H19 siRNA, miR-138 mimic or miR-138 inhibitor using the Lipofectamine® RNAiMAX kit (Thermo Fisher Scientific, Waltham, MA, USA). The CAL-27 cells were transfected with pcDNA-H19 or pcDNA-H19 plus miR-138 mimic using Lipofectamine® 2000 (Life Technologies) according to the manufacturer's instructions. The cells were harvested after 48 h and used for further analysis.

Lentivirus production and infection. Lentiviral constructs carrying shRNA targeting H19 (Lv-shRNA), and an empty negative control vector (LV-GFP) were obtained from GenePharma (Shanghai, China). The 293 cells (CRL-1573, ATCC) were co-transfected with Lenti-Pac HIV Expression Packaging Mix and the lentiviral vectors (or the control lentivirus vectors) using Lipofectamine 2000 (Life Technologies). After 48 h, lentiviral particles in the supernatant were harvested and ultra-centrifuged to concentrate the lentiviral particles. Subsequently, the HSC-2 and Ca9-22 cells grown on 6-well plates were transduced with the lentiviruses of 10 transduction units (TU) per cell. The expression of H19 in the transduced cells was examined by real-time PCR analysis.

Analysis of cell proliferation, apoptosis and cell cycle progression. Cell proliferation was examined by MTT assay according to the manufacturer's instructions (Roche Applied Science, Basel, Switzerland). Briefly, approximately $1x10^3$ cells were seeded in a 96-well culture plate for 24 h. The cells were then transfected with si-H19, si-Scramble, miR-138 inhibitor or miR-control. At various time points, 0.5 mg/ml MTT solution was added to each well. The absorbance was then recorded at 490 nm on a Bio-Rad model 680 microplate reader, (Bio-Rad Laboratories, Hercules, CA, USA). For the analysis of apoptosis, the cells were stained with Annexin V-FITC and propidium iodide (PI) (TACS Annexin V-FITC, Trevigen Inc., Gaithersburg, MD, USA) and then analyzed with double-label flow cytometry on a flow cytometer (FACSCanto II; BD Biosciences, San Jose, CA, USA). For cell cycle analysis, the cells were resuspended in PBS, stained with PI containing RNase A for 30 min at 37˚C, and analyzed by flow cytometry. All the assays were conducted in triplicate.

In vivo tumor growth assay. All animal procedures were performed according to national guidelines and approved by the Animal Care Ethics Committee of Shenzhen Hospital of Southern Medical University. Twenty female BALB/c nude mice (weighing 20±2 g; 4 weeks old, Laboratory Animal Center of Shanghai, Academy of Science) were used in this study. The HSC-2 and Ca9-22 cells transfected with Lv-shRNA or Lv-Control were injected into the left flanks of the nude mice ($2x10^6$ cells/mouse). After 5 weeks, the mice were sacrificed and tumor tissues were dissected. The tumor weight was measured and the tumor volume was calculated according to the following formula: (length x width^2)/2. The largest tumor size and volume in the mice of different groups was 1.30 g and 1,500 mm^3 (Lv-Control-transfected HSC-2 cells), 1.25 g and 1,700 mm^3 (Lv-Control transfected Ca9-22 cells), 0.68 g and 1,150 mm^3 (Lv-siRNA transfected HSC-2 cells), 0.73 g and 1,300 mm^3 (Lv- siRNA transfected Ca9-22 cells).

Bioinformatics. *In silico* prediction of miRNA binding sites within the H19 3'UTR was performed using TargetScan (www.targetscan.org) and PicTar (http://www.pictar.org).

Luciferase assays. The 3'-UTR of H19, with wild-type or mutant (Mut) binding sites for miR-138, was amplified and cloned into the pGL3 vector (Promega, Madison, WI, USA) to generate the plasmid pGL3-WT-H19-1 (wt-H9-1) or pGL3-WT-H19-2 (wt-H9-2). The putative binding site of miR-138 in H19 was mutated by using a QuikChange Site Directed Mutagenesis Kit (Agilent, Santa Clara, CA, USA) to synthetize mutant type pGL3-mut-H19-1 (Mut-H19-1) or pGL3-mut-H19-2 vector (Mut-H19-2). For the luciferase reporter assay, the 293 cells were co-transfected with the luciferase reporter vectors and miR-138 mimics or corresponding negative control (GenePharma) using Lipofectamine 2000 reagent (Life Technologies). The pRL-TK plasmid (Promega) was used as a normalizing control. After 48 h of incubation, luciferase activity was analyzed using the Dual-Luciferase Reporter Assay System (Promega) according to the manufacturer's instructions.

Wound healing assay. The cells were plated in 6-well plates and transfected when cultured to 95% confluence. The cell layers were then scratched using a 10 μl plastic pipette tip to produce wounds. The wounds were photographed at 0 and 48 h under an inverted phase contrast microscope (IX71; Olympus Corp., Tokyo, Japan). Three random fields were marked and measured. All the assays were carried out in triplicate.

Cell invasion assays. For invasion assays, a total of $3x10^4$ HSC-2 and Ca9-22 cells in 150 μl serum-free medium at post-transfection were seeded into the upper chamber (24-well insert, pore size 8 μm; Corning, NY, USA) pre-coated with 30 μg/well Matrigel solution (BD Biosciences), and the lower chambers were filled with 500 μl of 10% FBS medium. Following incubation at 37˚C for 48 h, the membranes were fixed with 4% polyoxymethylene and stained with 0.1% crystal violet (Sigma-Aldrich). Five pre-determined fields were counted under a microscope (Olympus Corp., original magnification, x200). All assays were performed in triplicate.

Western blot analysis. Total proteins were extracted from cells using radioimmunoprecipitation assay (RIPA) lysis buffer (Sigma-Aldrich) and quantified with a Bicin Choninic Acid (BCA) protein assay kit (Pierce, Rockford, IL, USA). A total of 40 μg of protein were subjected to 10% SDS-PAGE, and subsequently transferred onto a polyvinylidene difluoride membranes (Millipore, Billerica, MA, USA). The blots were incubated with the primary antibodies specific for cleaved caspase-3 (1:500; Cat. no. 9661), cleaved poly(ADP-ribose) polymerase (PARP; 1:1,000; Cat. no. 5625), Bax (1:1,000; Cat. no. 5023), EZH2 (1:1,000; Cat. no. 5246), zinc finger E-box-binding homeobox 1 (ZEB1; 1:1,000; Cat. no. 3396), E-cadherin (1:1,000; Cat. no. 14472), vimentin (1:1,000; Cat. no. 5741), N-cadherin (1:1,000; Cat. no. 13116) and β-actin (1:2,000; Cat. no. 4970). All antibodies were obtained from Cell Signaling Technology, Inc. (Danvers, MA, USA). Following 3 washes in TBST, the membranes were incubated with corresponding horseradish peroxidase (HRP)-conjugated secondary antibody (1:10,000; Santa Cruz Biotechnology, Inc.) for 2 h at room temperature, and washed with TBST 3 times. The protein bands were visualized by ECL detection reagent (GE Healthcare Life Sciences, Piscataway, NJ, USA). The intensity of the protein fragments was quantified with the Quantity One software (4.5.0 basic; Bio-Rad).

Statistical analysis. Statistical analyses were performed with GraphPad Prism 5 software (GraphPad Software, Inc.,

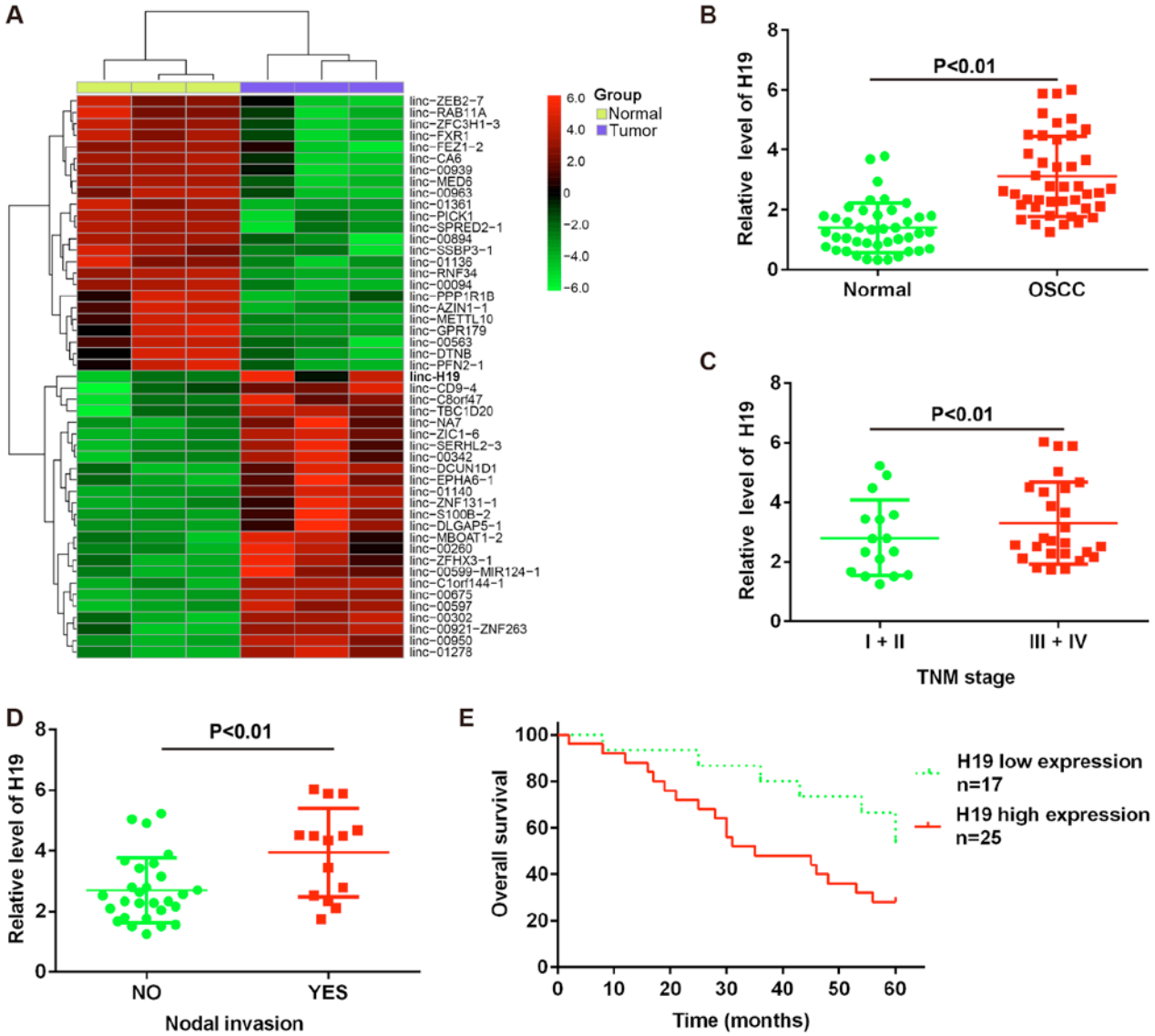

Figure 1. Long non-coding RNA (lncRNA) H19 is highly expressed in OSCC. (A) Hierarchical clustering analysis of 49 lncRNAs that were differentially expressed between OSCC tissues and non-tumor samples (>2.0-fold, P<0.05). Expression values are represented in shades of red and green indicating expression above and below the median expression value across all samples. (B) RT-qPCR was used to validate the expression of H19 in 42 paired OSCC and non-tumor samples. P<0.01 vs. normal group. (C) Expression level of H19 positively correlated with the tumor grade in OSCC. P<0.01 vs. I + II grades. (D) Expression level of H19 positively correlated with nodal invasion in OSCC (P<0.01). The x-axis shows the nodal status (NO or YES), and the y-axis represents H19 levels normalized against U6. (E) H19 expression was classified into 2 groups: H19 low expression group (n=17) and H19 high expression group (n=25). Kaplan-Meier analyses of the associations between the H19 expression level and overall survival of patients with OSCC (the log-rank test was used to calculate P-values).

La Jolla, CA, USA). All data are presented as the means ± SD. Differences were analyzed by a Student's t-test between two groups or one-way analysis of variance (ANOVA), followed by Tukey's multiple comparison tests between multiple groups. Spearman's analysis was used in correlation analysis. Survival analysis under the circumstance of Kaplan-Meier method. A P-value <0.05 was considered to indicate a statistically significant difference.

Results

lncRNA H1 is overexpressed in OSCC. To identify the lncRNAs involved in the development and progression of OSCC, a GSE dataset was obtained from the GEO database under the accession number GSE3524 (https://www.ncbi.nlm.nih.gov/geo/query/acc.cgi?acc=GSE3524). Analysis of these data revealed that 24 lncRNAs were downregulated and 25 miRNAs were upregulated in the tumor group, compared with the normal group. Among the aberrantly expressed lncRNAs, lncRNA H1 was the most significantly upregulated lncRNA in GSE dataset (Fig. 1A). To validate the microarray analysis finding, we detected H19 expression in a cohort of 42 paired tumor tissues and normal tissues. The detailed patient clinical data are presented in Table I. As shown in Fig. 1B, H19 expression was increased in tumor tissues compared with normal tissues. These data suggested that H19 may be involved in the process of carcinogenesis.

To determine whether H19 expression was associated with the grade of malignancy and nodal invasion in OSCC, we examined the expression level of H19. We demonstrated that H19 expression was positively associated with the pathological grades of OSCC and nodal invasion (Fig. 1C and D). Based

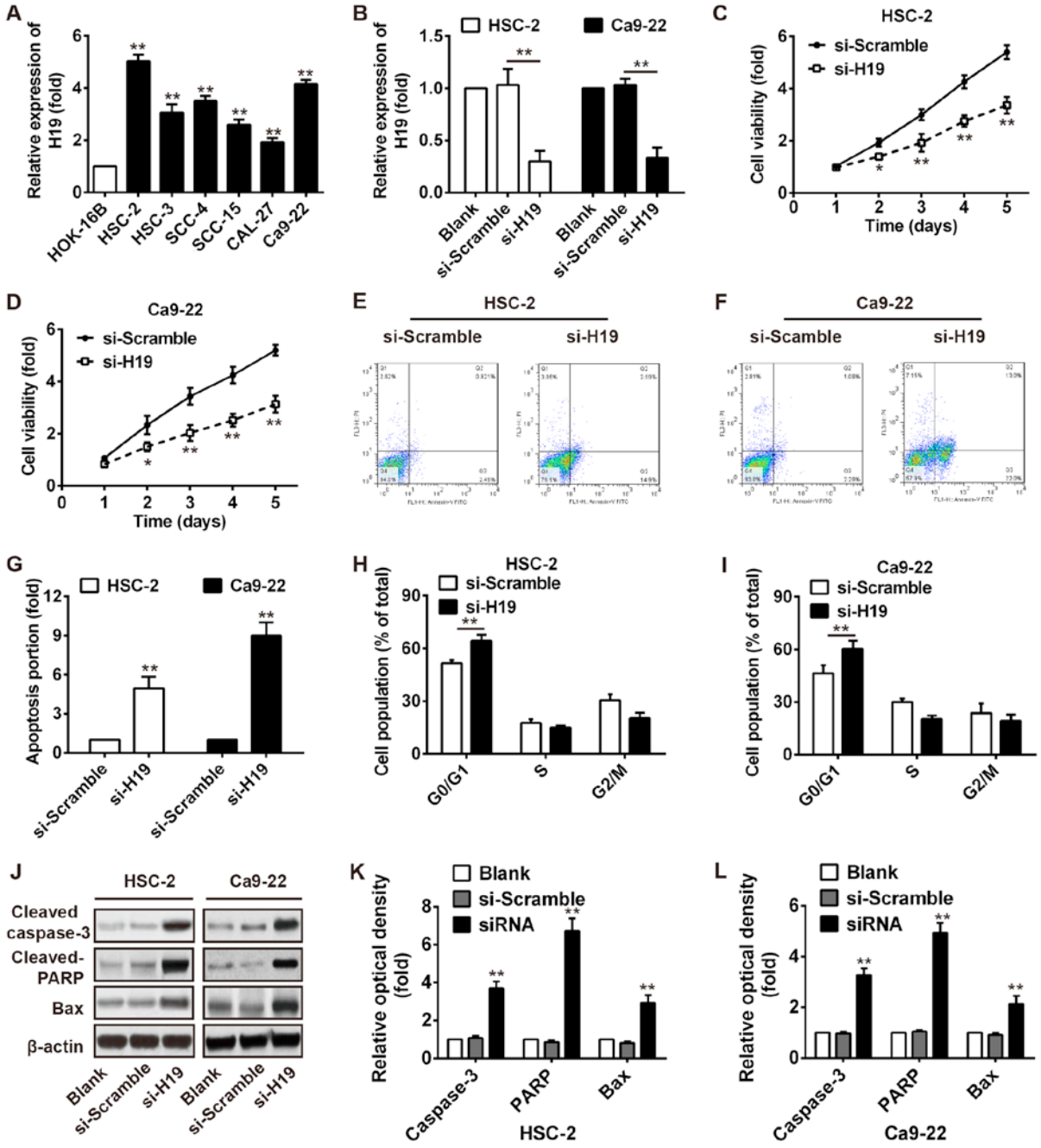

Figure 2. Effects of H19 on OSCC cell growth *in vitro*. (A) RT-qPCR analysis of H19 expression in OSCC cell lines. **P<0.01 vs. HOK-16B cells. (B) Relative expression levels of H19 in OSCC cells transfected with si-H19 or si-Scramble. **P<0.01 vs. si-Scramble group. (C and D) MTT assay was performed to determine the effects of transfection with si-H19 or si-Scramble on HSC-2 and Ca9-22 cell proliferation. *P<0.05 and **P<0.01 vs. si-Scramble group. (E-G) Annexin V/propidium iodide-double staining assay was performed to determine the apoptosis of HSC-2 and Ca9-22 cells transfected with si-H19 or si-Scramble. **P<0.01 vs. si-Scramble group. (H and I) The percentage of cells in the G0/G1 phase was increased in cells in which H19 was knocked down (HSC-2 and Ca9-22 cells). **P<0.01 vs. si-Scramble group. (J-L) Relative expression of apoptosis-related protein levels, including caspase-3, PARP and Bax in the HSC-2 and Ca9-22 cells following transfection with si-H19 or si-Scramble. **P<0.01 vs. si-Scramble group.

on the relative expression ratios of <0.5, the 42 clinical cases were divided into 2 groups as follows: the H19 low expression group (n=17) and the H19 high expression group (n=25). We then assessed whether the expression of H19 correlated with the post-operative survival time of patients with OSCC. Kaplan-Meier survival analysis revealed that patients with a high H19 expression had a poorer overall survival than those with a low H19 expression (Fig. 1E). Taken together, these findings indicate that H19 may be used as a biomarker for the diagnosis and prognosis of OSCC.

Knockdown of H19 inhibits the proliferation, increases the G0/G1 phase population and induces the apoptosis of OSCC cells. To examine the effect of H19 on cell growth, we first measured the expression levels of H19 in 6 OSCC cell lines (HSC-2, HSC-3, SCC-4, SCC-15, CAL-27 and Ca9-22) and a normal oral mucosa cell line (HOK-16B). As shown in Fig. 2A, a higher expression of H19 was observed in the OSCC cell lines compared with the normal oral mucosa cell line, particularly in the HSC-2 and Ca9-22 cells. Subsequently, the HSC-2 and Ca9-22 cells were transiently transfected with si-H19 and the

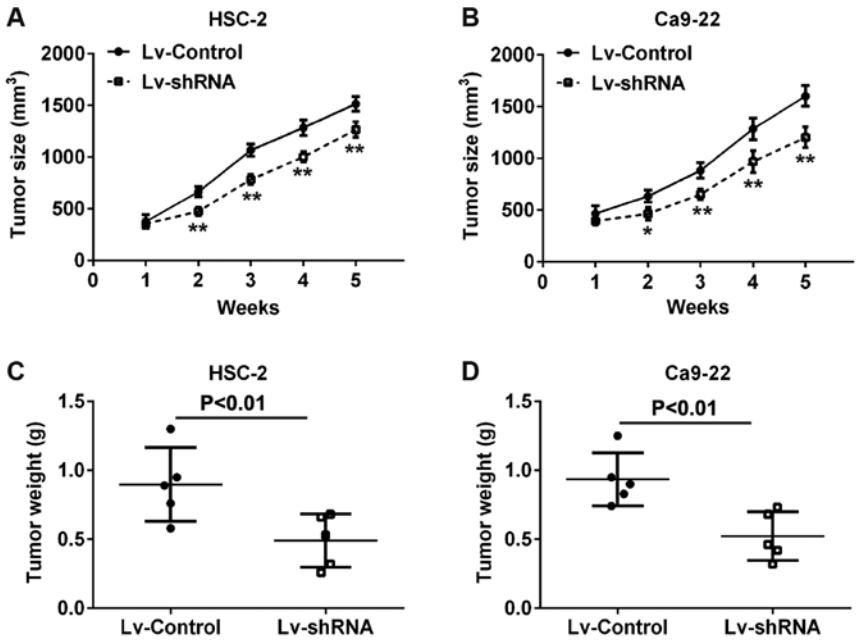

Figure 3. Knockdown of H19 inhibits tumor growth *in vivo*. Lv-Control or Lv-shRNA was infected into the HSC-2 and Ca9-22 cells, which were injected into nude mice. (A and B) Tumor sizes were measured each week following the Lv-shRNA injection (5 mice/group). *P<0.05 and **P<0.01 vs. Lv-Control group. (C and D) Tumor weights were measured after the Lv-shRNA injection (5 mice/group). P<0.01 vs. Lv-Control group.

Table I. Clinicopathogical characteristics of the study subjects.

Characteristic	n (%)
Sex	
Male	33 (78.57)
Female	9 (21.43)
Age (years)	
≥50	31 (73.81)
<50	11 (26.19)
Tobacco use	
Yes	32 (76.19)
No	10 (23.81)
Alcohol use	
Yes	30 (71.43)
No	12 (28.57)
Tumor site	
Tongue	23 (54.76)
Floor of mouth	8 (19.05)
Alveolar	6 (14.29)
Buccal mucosa	4 (9.52)
Retromolar	1 (2.38)
Tumor stage	
I-II	16 (38.10)
III-IV	26 (61.90)
Differentiation	
Well and moderate	34 (80.95)
Poor	8 (19.05)
Nodal invasion	
Negative	28 (66.67)
Positive	14 (33.33)

endogenous level of H19 was effectively decreased (Fig. 2B). As demonstrated by MTT assays, we found that H19 silencing significantly decreased the viability of the HSC-2 and Ca9-22 cells (Fig. 2C and D). Furthermore, the proportion of the cell population undergoing apoptosis was increased after knockdown of H19 in the HSC-2 and Ca9-22 cells (Fig. 2E-G). Flow cytometry also revealed a significant promotion of cells in the G0/G1 phase of the cell cycle in the HSC-2 and Ca9-22 cells transfected with si-H19 (Fig. 2H and I). In addition, western blot analysis revealed that the expression levels of apoptosis-related proteins, including cleaved caspase-3 and cleaved PARP and Bax were markedly increased after H19 knockdown (Fig. 2J-L). Our results thus revealed that H19 knockdown inhibited several malignancy-related parameters of OSCC *in vitro*.

Knockdown of H19 inhibits tumor growth in vivo. To evaluate the functional roles of H19 *in vivo*, we established a xenograft mouse mode in which Lv-shRNA or Lv-Control-transfected HSC-2 and Ca9-22 cells were transplanted into the flanks of BALB/c nude mice. Consistent with the results obtained *in vitro*, after 5 weeks, tumor volumes in the mice injected with cells from the si-H19 group were markedly smaller compared with those in the mice injected with cells from the Lv-Control (Fig. 3A and B). Similarly, tumor weights in the mice injected with cells from the Lv-shRNA group were significantly lower compared with those in the mice injected with cells from the Lv-Control group (Fig. 3C and D). These results indicate that the knockdown of H19 expression inhibits tumor growth *in vivo*.

Knockdown of H19 inhibits the migration and invasion of OSCC cells. Based on the above-mentioned results in that the expression of H19 was higher in metastatic tissues, we hypothesized that H19 may be associated with the metastasis

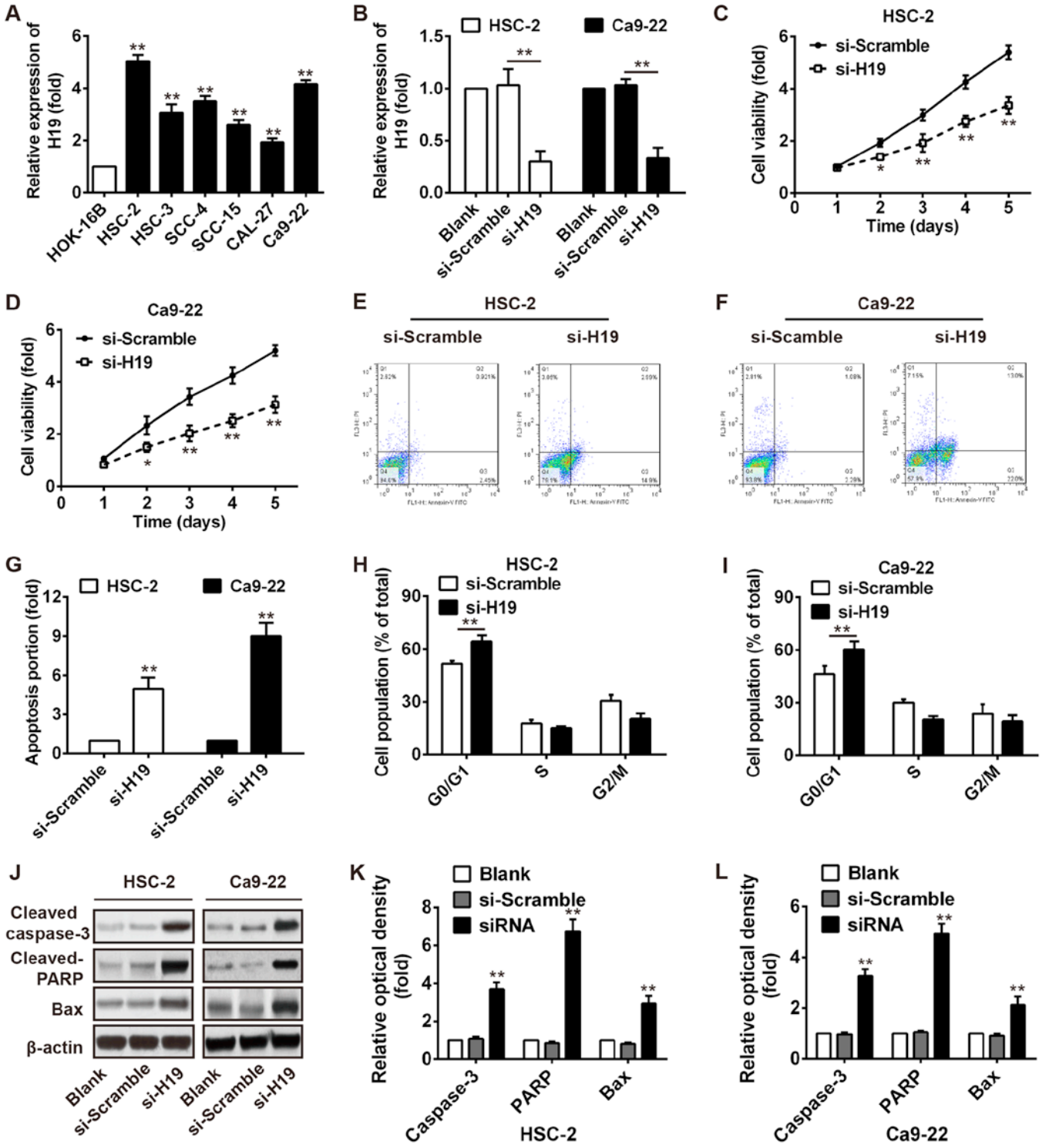

Figure 4. Knockdown of H19 inhibits the migration and invasion of OSCC cells. (A) Wound healing assay was carried out to evaluate the effect of H19 on the migration of HSC-2 and Ca9-22 cells. **P<0.01 vs. si-Scramble group. (B) Invasion assay (with Matrigel Transwell chambers) for investigating cell invasiveness. **P<0.01 vs. si-Scramble group. (C) Relative expression of EMT-related protein levels in HSC-2 and Ca9-22 cells following transfection with si-H19 and si-Scramble. **P<0.01 vs. si-Scramble group. Data are presented as the means ± SD from 3 independent experiments.

of OSCC. Thus, wound healing and Transwell assays were performed to examine the effects of H19 on OSCC cell metastasis. As shown in Fig. 4A, H19 silencing markedly inhibited the migration of monolayer-cultured HSC-2 and Ca9-22 cells. In addition, the numbers of invaded cells were markedly attenuated in the cells in which H19 was knocked down compared with the control cells (Fig. 4B). It is well known that EMT plays a critical role in the invasion and metastasis of OSCC cells (27). In this study, we thus assessed the effect of H19 on the expression of EMT related-genes. Our results demonstrated that H19 silencing significantly decreased the expression levels of vimentin and N-cadherin (mesenchymal markers), but increased the expression levels of ZEB1 and E-cadherin (epithelial markers) (Fig. 4C). These data suggest

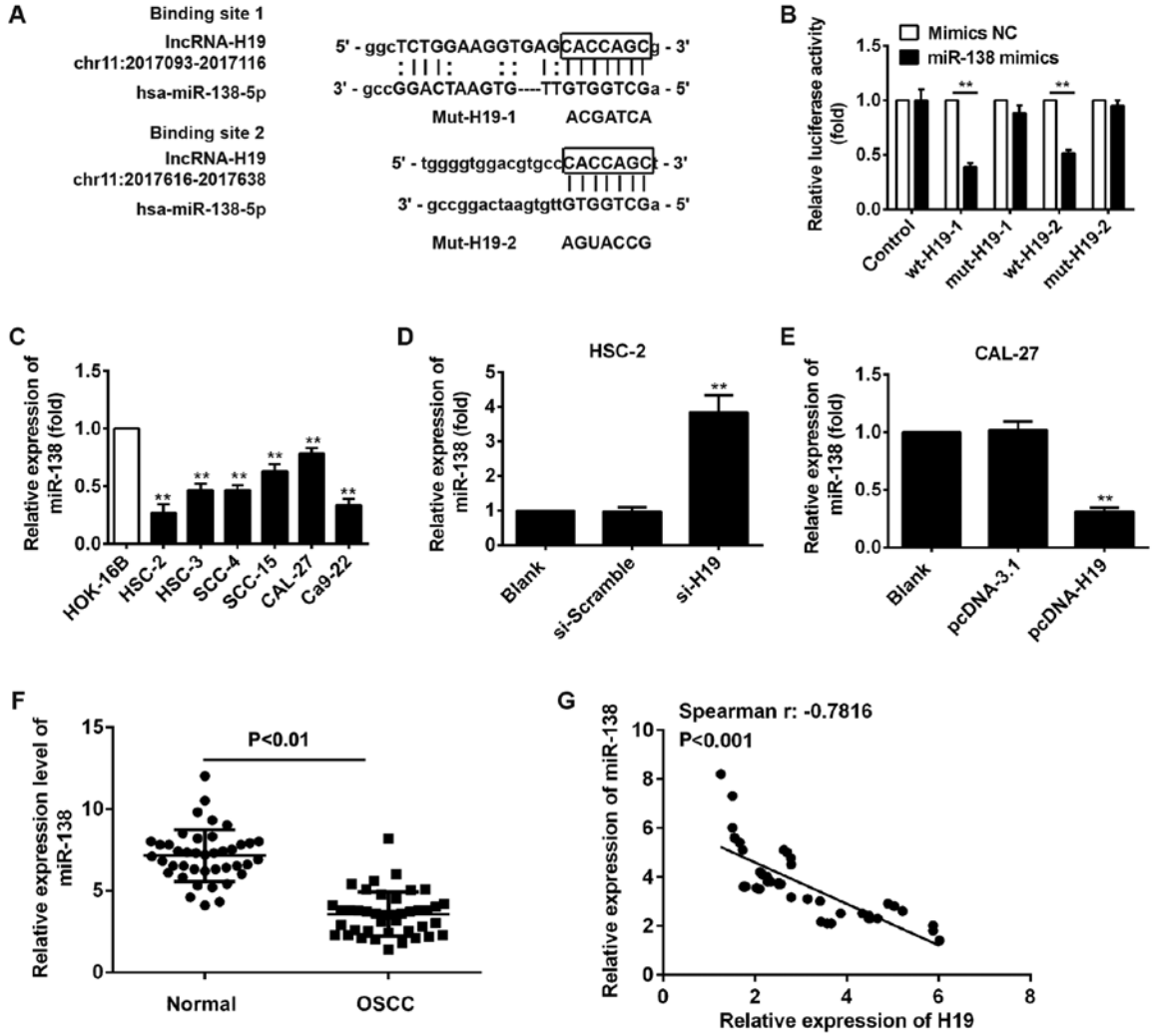

Figure 5. H19 directly inhibits miR-138 expression in OSCC. (A) The predicted miR-138 binding sites on H19. (B) Luciferase activity in 293 cells co-transfected with miR-138 mimics and luciferase reporters containing wt-H19 or mut-H19 transcript. **P<0.01 vs. miR-138 mimic group. (C) miR-138 expression was validated in OSCC cell lines by RT-qPCR. **P<0.01 vs. HOK-16B group. (D) RT-qPCR analysis of miR-138 expression in HSC-2 cells transfected with si-H19 or si-Scramble. **P<0.01 vs. si-Scramble group. (E) RT-qPCR analysis of miR-138 expression in CAL-27 cells transfected with pcDNA-H19 or pcDNA3.1 plasmids. **P<0.01 vs. pcDNA3.1 group. (F) miR-138 expression was validated in OSCC tissues and corresponding adjacent normal tissues by RT-qPCR (P<0.01 vs. normal group). (G) Pearson's correlation analysis was performed to analyze the correlations between H19 and miR-138 expression in OSCC tissues (r=-0.7816; P<0.001).

that the knockdown of H19 suppresses OSCC cell metastasis by inhibiting EMT.

H19 directly targets miR-138 and inhibits its level in OSCC cells. Recently, studies have confirmed that lncRNAs can function as ceRNAs or molecular sponges that modulate miRNAs in cancers (28,29). In this study, we thus performed bioinformatics analysis using TargetScan and PicTar, and found that miR-138 contains a binding site for H19. The predicted binding sites for H19 in the miR-138 sequence are illustrated in Fig. 5A. To examine whether H19 directly targets miR-138, we conducted a luciferase assay. As shown in Fig. 5B, luciferase activity was significantly inhibited when wt-H19-1 or wt-H19-2 was co-transfected with miR-138 mimics compared with that after mimic NC co-transfection, whereas the inhibitory effect was abolished when the H19 3'-UTR was mutated. This indicated that miR-138 probably interacted with H19.

It has been found that miR-138 functions as a tumor suppressor in human OSCC (23). Thus, we first measured miR-138 expression in 6 OSCC cell lines (HSC-2, HSC-3, SCC-4, SCC-15, CAL-27 and Ca9-22) and a normal oral mucosa cell line (HOK-16B). Consistent with the findings previous of that study, the expression of miR-138 was also expressed at low levels in the OSCC cell lines, particularly in the HSC-2 and Ca9-22 cells (Fig. 5C). To further determine whether H19 affects OSCC cell proliferation and metastasis by regulating miR-138 expression, we measured miR-138 expression after the silencing or overexpression of H19 in HSC-2 and CAL-27 cells, and the results of RT-qPCR indicated that miR-138 expression was upregulated after the knockdown of H19 in the HSC-2 cells (Fig. 5D), whereas the miR-138 level was downregulated after H19 was overexpressed in the CAL-27 cells (Fig. 5E). Furthermore, we detected miR-138 expression in 42 pairs of OSCC tissues and normal tissues. Consistent with the results obtained with the OSCC cell lines, the expression of miR-138 was downregulated in the OSCC tissues (Fig. 5F), and an inverse correlation was observed between the expression of miR-138 and the expression of H19

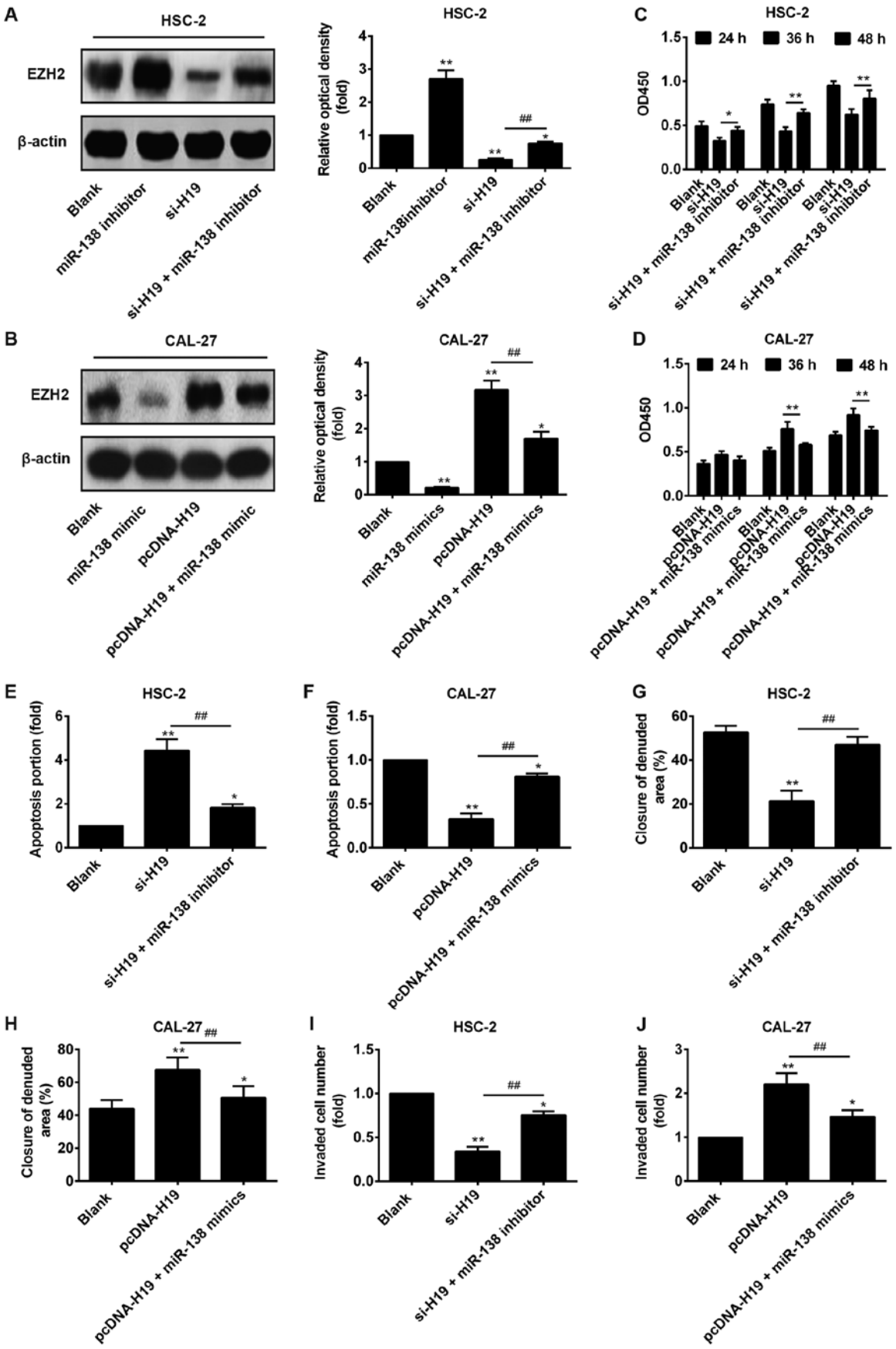

Figure 6. H19 regulates EZH2 by sponging miR-138 in OSCC cells. si-H19 and miR-138 inhibitor were transfected into HSC-2 cells, pcDNA-H19 and miR-138 mimic were transfected into CAL-27 cells. (A and B) Western blot analysis was performed to determine the expression of EZH2 in HSC-2 and CAL-27 cells. (C and D) MTT assay was performed to examine the proliferation of HSC-2 and CAL-27 cells. (E and F) Flow cytometric assay was performed to examine the apoptosis of HSC-2 and CAL-27 cells. (G and H) Wound healing assay was performed to determine the percentage of wound closure in the HSC-2 and CAL-27 cells. (I and J) Transwell invasion assay was performed to determine the numbers of invaded HSC-2 and CAL-27 cells. *P<0.05 and **P<0.01 vs. blank group; $^{\#\#}$P<0.01 vs. si-H19 group or pcDNA H1 group.

(Fig. 5G). All these data suggest that H19 negatively regulates the expression of miR-138 in OSCC.

Suppression of miR-138 attenuates the si-H19-induced inhibitory effects on OSCC cells by targeting EZH2. Recent findings have demonstrated that EZH2 acts as an oncogene and correlates with the malignant potential and a poor prognosis in a wide range of cancer types, including OSCC (30-32). Importantly, EZH2 has been identified as a target of miR-138 in several cancer cells (33-35). Therefore, we sought to determine whether H19 functions as a ceRNA for miR-138 to regulate the expression of EZH2 in OSCC. Western blot analysis revealed that the knockdown of H19 in the HSC-2 cells significantly decreased the expression levels of EZH2, while transfection with miR-138 inhibitor restored EZH2 expression in the OSCC cells in which H19 was knocked down (Fig. 6A). By contrast, the overexpression of H19 in the CAL-27 cells increased the expression levels of EZH2, while transfection with miR-138 mimic inhibited the promotion of EZH2 expression in the cells overexpressing H19 (Fig. 6B). These results suggest that H19 regulates the expression of the oncogene EZH2 by competing with miR-138 in OSCC cells.

In order to analyze the importance of miR-138 in H19-mediated OSCC proliferation, apoptosis and invasion, we knocked down the expression of miR-138 in the HSC-2 cells transfected with si-H19 and overexpressed its expression in the CAL-27 cells transfected with pcDNA-H19, separately. The results revealed that miR-138 knockdown blocked the inhibitory effects of H19 on cell proliferation, apoptosis and invasion (Fig. 6C-J), suggesting that the effects of H19 on OSCC growth and invasion are partially mediated by miR-138. Taken together, these data indicated that the effects of H19 on the growth and metastasis of OSCC are partially mediated by regulating the expression of miR-138.

Discussion

In the present study, we found that lncRNA H1 was upregulated in OSCC tissues and cell lines and that a high H19 expression was associated with a poor clinical outcome. Moreover, the knockdown of H19 inhibited OSCC cell proliferation, migration and invasion, induced cell apoptosis and decreased the tumor growth *in vivo*. Mechanistically, we demonstrated that H19 affects the the biological characteristics of OSCC cells by positively modulating EZH2 expression through competition for miR-138. Collectively, our results demonstrated the roles and functional mechanisms of H19 in OSCC and provide novel insight into potential therapeutic targets for OSCC.

Recent experimental studies have demonstrated that lncRNAs play various roles in tumorigenesis, including OSCC (36-40). For example, HOX transcript antisense RNA (HOTAIR) has been reported to be upregulated in OSCC and its expression has been shown to be associated with the metastasis and poor prognosis of OSCC (41). Metastasis associated lung adenocarcinoma transcript 1 (MALAT1) is another reported lncRNA, which contributes to EMT-mediated metastasis in OSCC by modulating the activation of β-catenin and NF-κB pathways (42). However, the roles of lncRNAs in OSCC remain largely unknown. In this study, we analyzed and validated a list of significantly dysregulated lncRNAs in OSCC tissues by retrieving the microarray data in the GEO dataset (accession no. GSE3524). In this study, we found that lncRNA H1 was one of the most significantly differentially expressed lncRNA. Moreover, a high level of H19 positively correlated with clinical stages and was identified as a prognostic parameter for patient survival. These data indicate that H19 may serve as a biomarker for the diagnosis and prognosis of OSCC.

A large body of evidence has indicated that H19 is involved in cancer invasion and metastasis. In esophageal squamous cell carcinoma (ESCC), H19 has been shown to be upregulated and to promote cell proliferation and metastasis (43). Xu *et al* found that H19 functioned as a marker of poor prognosis in cholangiocarcinoma (CCA) and H19 enhanced cell migration and invasion by affecting EMT (44). H19 can also activate Wnt/β-catenin signaling to affect cell proliferation and metastasis in bladder cancer (45). In this study, we proved that the knockdown of H19 inhibited OSCC cell proliferation, migration and invasion, induced cell apoptosis, arrested the cells in the G0/G1 phase and decreased the tumor volume *in vivo*. Accordingly, apoptosis was increased, conferred by the upregulation of cleaved caspase-3, cleaved PARP and Bax. Moreover, we found that the ectopic expression of H19 decreased the expression of E-cadherin and ZEB1, and increased the expression of vimentin and N-cadherin in OSCC cells, which suggested that H19 may promote OSCC cell invasion by inducing EMT. Therefore, these data suggest that H19 may serve as an oncogene that promotes OSCC malignant progression.

Recently, increasing evidence has indicated that lncRNAs function as ceRNAs to silence target mRNAs by sponging target miRNAs (46,47). Sui *et al* found that lncRNA GIHCG promoted hepatocellular carcinoma progression by epigenetically regulating miR-200b/a/429 (48). Another study demonstrated that lncRNA PVT1 promoted cervical cancer progression through the silencing of miR-200b (49). Similarly, lncRNA H1 competitively binds miR-17-5p to regulate YES1 expression in thyroid cancer (50). In this study, we demonstrated that H19 directly targeted miR-138 by bioinformatics analysis and luciferase reporter assays. We also confirmed that miR-138 was significantly decreased in OSCC tissues and inversely correlated with the expression level of H19. However, the ceRNA mechanisms for H19 deregulation in OSCC have not been thoroughly elucidated.

Previous studies have indicated that miR-138 plays critical roles in various types of cancer by targeting EZH2. For example, miR-138 acts as a tumor suppressor miRNA in human clear cell renal cell carcinoma (ccRCC), induces SN-12 cell senescence by downregulating EZH2 expression (34). The study by Zhang *et al* demonstrated that miR-138 inhibited tumor growth through the repression of EZH2 in non-small cell lung cancer (51). A recent study identified EZH2 as a target of miR-138 in osteosarcoma cells (33). In addition, Li *et al* found that lncRNA H1 regulated EZH2 expression by interacting with miR-630 and promoted cell invasion in nasopharyngeal carcinoma (52). Therefore, it was hypothesized that H19 may also serve as a ceRNA to regulate EZH2 expression by sponging miR-138. Consistent with the findings of previous studies, we confirmed that H19 regulated the expression of EZH2, and that miR-138 attenuated the effects

of H19 on the expression of EZH2 in OSCC cells. Notably, all the effects of H19 on the biological characteristics of the OSCC cells were blocked by miR-138. Taken together, these data strongly suggest that lncRNA H1 functions as a ceRNA for miR-138 in OSCC.

In this study, the detection of H19 level in OSCC cell lines indicated that H19 had the highest level in HSC-2 cells and the lowest level in CAL-27 cells. Therefore, the HSC-2 cells were selected for the loss-of-function experiments and the CAL-27 cells for gain-of-function experiments. The results revealed that the knockdown of H19 inhibited OSCC cell proliferation and invasion, and induced cell apoptosis, whereas the overexpression of H19 had an opposite result. In addition, the expression of H19 in 6 OSCC cell lines was markedly upregulated compared with that in the HOK-16B cells. However, we did not find OSCC tumor cells in which the expression of H19 was similar to that in the HOK-16B cells. In the future, we aim to find a cell line with which to explore whether this approach would yield the same results in normal H-19-expressing cells in which H19 is knocked down or overexpressed.

In conclusion, in this study, demonstrate that H19 promotes EZH2 expression by competitively binding miR-138, contributing to the induction of the EMT process in OSCC. We also identified the H19/miR-138/EZH2 axis as a novel signaling network in OSCC, which may provide a novel therapeutic strategy for the targeted treatment of OSCC.

References

1. Siegel R, Ma J, Zou Z and Jemal A: Cancer statistics, 2014. CA Cancer J Clin 64: 9-29, 2014.
2. Chi AC, Day TA and Neville BW: Oral cavity and oropharyngeal squamous cell carcinoma - an update. CA Cancer J Clin 65: 401-421, 2015.
3. Kang YY, Sun FL, Zhang Y and Wang Z: SIRT1 acts as a potential tumor suppressor in oral squamous cell carcinoma. J Chin Med Assoc S1726-4901(17)30270-8, 2017.
4. Sharma A, Boaz K and Natarajan S: Understanding patterns of invasion: A novel approach to assessment of podoplanin expression in prediction of lymph node metastasis in OSCC. Histopathology, 2017.
5. Rao SJ, Rao JBM and Rao PJ: Immunohistochemical analysis of stromal fibrocytes and myofibroblasts to envision the invasion and lymph node metastasis in oral squamous cell carcinoma. J Oral Maxillofac Pathol 21: 218-223, 2017.
6. Carninci P, Kasukawa T, Katayama S, Gough J, Frith MC, Maeda N, Oyama R, Ravasi T, Lenhard B, Wells C, *et al*; RIKEN Genome Exploration Research Group and Genome Science Group (Genome Network Project Core Group): The transcriptional landscape of the mammalian genome. Science 309: 1559-1563, 2005.
7. Krzyzanowski PM, Muro EM and Andrade-Navarro MA: Computational approaches to discovering noncoding RNA. Wiley Interdiscip Rev RNA 3: 567-579, 2012.
8. Rinn JL and Chang HY: Genome regulation by long noncoding RNAs. Annu Rev Biochem 81: 145-166, 2012.
9. Batista PJ and Chang HY: Long noncoding RNAs: Cellular address codes in development and disease. Cell 152: 1298-1307, 2013.
10. Wang L, Zhao Z, Feng W, Ye Z, Dai W, Zhang C, Peng J and Wu K: Long non-coding RNA TUG1 promotes colorectal cancer metastasis via EMT pathway. Oncotarget 7: 51713-51719, 2016.
11. Guttman M, Donaghey J, Carey BW, Garber M, Grenier JK, Munson G, Young G, Lucas AB, Ach R, Bruhn L, *et al*: lincRNAs act in the circuitry controlling pluripotency and differentiation. Nature 477: 295-300, 2011.
12. Gupta RA, Shah N, Wang KC, Kim J, Horlings HM, Wong DJ, Tsai MC, Hung T, Argani P, Rinn JL, *et al*: Long non-coding RNA HOTAIR reprograms chromatin state to promote cancer metastasis. Nature 464: 1071-1076, 2010.
13. Ariel I, Ayesh S, Perlman EJ, Pizov G, Tanos V, Schneider T, Erdmann VA, Podeh D, Komitowski D, Quasem AS, *et al*: The product of the imprinted H19 gene is an oncofetal RNA. Mol Pathol 50: 34-44, 1997.
14. Berteaux N, Lottin S, Monté D, Pinte S, Quatannens B, Coll J, Hondermarck H, Curgy JJ, Dugimont T and Adriaenssens E: H19 mRNA-like noncoding RNA promotes breast cancer cell proliferation through positive control by E2F1. J Biol Chem 280: 29625-29636, 2005.
15. Matouk IJ, DeGroot N, Mezan S, Ayesh S, Abu-lail R, Hochberg A and Galun E: The H19 non-coding RNA is essential for human tumor growth. PLoS One 2: e845, 2007.
16. Ma C, Nong K, Zhu H, Wang W, Huang X, Yuan Z and Ai K: H19 promotes pancreatic cancer metastasis by derepressing let-7's suppression on its target HMGA2-mediated EMT. Tumour Biol 35: 9163-9169, 2014.
17. Liang WC, Fu WM, Wong CW, Wang Y, Wang WM, Hu GX, Zhang L, Xiao LJ, Wan DC, Zhang JF, *et al*: The lncRNA H1 promotes epithelial to mesenchymal transition by functioning as miRNA sponges in colorectal cancer. Oncotarget 6: 22513-22525, 2015.
18. Guo QY, Wang H and Wang Y: lncRNA H1 polymorphisms associated with the risk of OSCC in Chinese population. Eur Rev Med Pharmacol Sci 21: 3770-3774, 2017.
19. Zhang DM, Lin ZY, Yang ZH, Wang YY, Wan D, Zhong JL, Zhuang PL, Huang ZQ, Zhou B and Chen WL: lncRNA H1 promotes tongue squamous cell carcinoma progression through β-catenin/GSK3β/EMT signaling via association with EZH2. Am J Transl Res 9: 3474-3486, 2017.
20. Bartel DP: MicroRNAs: Genomics, biogenesis, mechanism, and function. Cell 116: 281-297, 2004.
21. Zeng G, Xun W, Wei K, Yang Y and Shen H: MicroRNA-27a-3p regulates epithelial to mesenchymal transition via targeting YAP1 in oral squamous cell carcinoma cells. Oncol Rep 36: 1475-1482, 2016.
22. Wu B, Lei D, Wang L, Yang X, Jia S, Yang Z, Shan C, Yang X, Zhang C and Lu B: miRNA-101 inhibits oral squamous-cell carcinoma growth and metastasis by targeting zinc finger E-box binding homeobox 1. Am J Cancer Res 6: 1396-1407, 2016.
23. Xu R, Zeng G, Gao J, Ren Y, Zhang Z, Zhang Q, Zhao J, Tao H and Li D: miR-138 suppresses the proliferation of oral squamous cell carcinoma cells by targeting Yes-associated protein 1. Oncol Rep 34: 2171-2178, 2015.
24. Toruner GA, Ulger C, Alkan M, Galante AT, Rinaggio J, Wilk R, Tian B, Soteropoulos P, Hameed MR, Schwalb MN, *et al*: Association between gene expression profile and tumor invasion in oral squamous cell carcinoma. Cancer Genet Cytogenet 154: 27-35, 2004.
25. Livak KJ and Schmittgen TD: Analysis of relative gene expression data using real-time quantitative PCR and the 2(-Delta Delta C(T)) Method. Methods 25: 402-408, 2001.
26. Kuo HF, Liu PL, Chong IW, Liu YP, Chen YH, Ku PM, Li CY, Chen HH, Chiang HC, Wang CL, *et al*: Pigment epithelium-derived factor mediates autophagy and apoptosis in myocardial hypoxia/reoxygenation injury. PLoS One 11: e0156059, 2016.
27. Li YC, Bu LL, Mao L, Ma SR, Liu JF, Yu GT, Deng WW, Zhang WF and Sun ZJ: SATB1 promotes tumor metastasis and invasiveness in oral squamous cell carcinoma. Oral Dis 23: 247-254, 2017.
28. Qu J, Li M, Zhong W and Hu C: Competing endogenous RNA in cancer: A new pattern of gene expression regulation. Int J Clin Exp Med 8: 17110-17116, 2015.
29. Wang H, Shen Q, Zhang X, Yang C, Cui S, Sun Y, Wang L, Fan X and Xu S: The long non-coding RNA XIST controls non-small cell lung cancer proliferation and invasion by modulating miR-186-5p. Cell Physiol Biochem 41: 2221-2229, 2017.
30. Sauvageau M and Sauvageau G: Polycomb group proteins: Multi-faceted regulators of somatic stem cells and cancer. Cell Stem Cell 7: 299-313, 2010.
31. Su KJ, Lin CW, Chen MK, Yang SF and Yu YL: Effects of EZH2 promoter polymorphisms and methylation status on oral squamous cell carcinoma susceptibility and pathology. Am J Cancer Res 5: 3475-3484, 2015.
32. Kidani K, Osaki M, Tamura T, Yamaga K, Shomori K, Ryoke K and Ito H: High expression of EZH2 is associated with tumor proliferation and prognosis in human oral squamous cell carcinomas. Oral Oncol 45: 39-46, 2009.
33. Zhu Z, Tang J, Wang J, Duan G, Zhou L and Zhou X: miR-138 acts as a tumor suppressor by targeting EZH2 and enhances cisplatin-induced apoptosis in osteosarcoma cells. PLoS One 11: e0150026, 2016.

34. Liang J, Zhang Y, Jiang G, Liu Z, Xiang W, Chen X, Chen Z and Zhao J: miR-138 induces renal carcinoma cell senescence by targeting EZH2 and is downregulated in human clear cell renal cell carcinoma. Oncol Res 21: 83-91, 2013.
35. Liu Q, Huang J, Zhou N, Zhang Z, Zhang A, Lu Z, Wu F and Mo YY: lncRNA loc285194 is a p53-regulated tumor suppressor. Nucleic Acids Res 41: 4976-4987, 2013.
36. Gutschner T and Diederichs S: The hallmarks of cancer: A long non-coding RNA point of view. RNA Biol 9: 703-719, 2012.
37. Gibb EA, Vucic EA, Enfield KS, Stewart GL, Lonergan KM, Kennett JY, Becker-Santos DD, MacAulay CE, Lam S, Brown CJ, *et al*: Human cancer long non-coding RNA transcriptomes. PLoS One 6: e25915, 2011.
38. Meng J, Li P, Zhang Q, Yang Z and Fu S: A four-long non-coding RNA signature in predicting breast cancer survival. J Exp Clin Cancer Res 33: 84, 2014.
39. Zhou M, Zhao H, Wang Z, Cheng L, Yang L, Shi H, Yang H and Sun J: Identification and validation of potential prognostic lncRNA biomarkers for predicting survival in patients with multiple myeloma. J Exp Clin Cancer Res 34: 102, 2015.
40. Yang YT, Wang YF, Lai JY, Shen SY, Wang F, Kong J, Zhang W and Yang HY: Long non-coding RNA UCA1 contributes to the progression of oral squamous cell carcinoma by regulating the WNT/β-catenin signaling pathway. Cancer Sci 107: 1581-1589, 2016.
41. Wu Y, Zhang L, Zhang L, Wang Y, Li H, Ren X, Wei F, Yu W, Liu T, Wang X, *et al*: Long non-coding RNA HOTAIR promotes tumor cell invasion and metastasis by recruiting EZH2 and repressing E-cadherin in oral squamous cell carcinoma. Int J Oncol 46: 2586-2594, 2015.
42. Zhou X, Liu S, Cai G, Kong L, Zhang T, Ren Y, Wu Y, Mei M, Zhang L and Wang X: Long non coding RNA MALAT1 promotes tumor growth and metastasis by inducing epithelial-Mesenchymal transition in oral squamous cell carcinoma. Sci Rep 5: 15972, 2015.
43. Tan D, Wu Y, Hu L, He P, Xiong G, Bai Y and Yang K: Long noncoding RNA H1 is up-regulated in esophageal squamous cell carcinoma and promotes cell proliferation and metastasis. Dis Esophagus 30: 1-9, 2017.
44. Xu Y, Wang Z, Jiang X and Cui Y: Overexpression of long noncoding RNA H1 indicates a poor prognosis for cholangiocarcinoma and promotes cell migration and invasion by affecting epithelial-mesenchymal transition. Biomed Pharmacother 92: 17-23, 2017.
45. Luo M, Li Z, Wang W, Zeng Y, Liu Z and Qiu J: Long non-coding RNA H1 increases bladder cancer metastasis by associating with EZH2 and inhibiting E-cadherin expression. Cancer Lett 333: 213-221, 2013.
46. Kallen AN, Zhou XB, Xu J, Qiao C, Ma J, Yan L, Lu L, Liu C, Yi JS, Zhang H, *et al*: The imprinted H19 lncRNA antagonizes let-7 microRNAs. Mol Cell 52: 101-112, 2013.
47. Tay Y, Kats L, Salmena L, Weiss D, Tan SM, Ala U, Karreth F, Poliseno L, Provero P, Di Cunto F, *et al*: Coding-independent regulation of the tumor suppressor PTEN by competing endogenous mRNAs. Cell 147: 344-357, 2011.
48. Sui CJ, Zhou YM, Shen WF, Dai BH, Lu JJ, Zhang MF and Yang JM: Long noncoding RNA GIHCG promotes hepatocellular carcinoma progression through epigenetically regulating miR-200b/a/429. J Mol Med (Berl) 94: 1281-1296, 2016.
49. Zhang S, Zhang G and Liu J: Long noncoding RNA PVT1 promotes cervical cancer progression through epigenetically silencing miR-200b. APMIS 124: 649-658, 2016.
50. Liu L, Yang J, Zhu X, Li D, Lv Z and Zhang X: Long noncoding RNA H1 competitively binds miR-17-5p to regulate YES1 expression in thyroid cancer. FEBS J 283: 2326-2339, 2016.
51. Zhang H, Zhang H, Zhao M, Lv Z, Zhang X, Qin X, Wang H, Wang S, Su J, Lv X, *et al*: miR-138 inhibits tumor growth through repression of EZH2 in non-small cell lung cancer. Cell Physiol Biochem 31: 56-65, 2013.
52. Li X, Lin Y, Yang X, Wu X and He X: Long noncoding RNA H1 regulates EZH2 expression by interacting with miR-630 and promotes cell invasion in nasopharyngeal carcinoma. Biochem Biophys Res Commun 473: 913-919, 2016.